



## CFD-based prognosis of hydrate dissociation inside X-mas tree with slickline intervention

Luiz Fernando B. Nardi<sup>1</sup>, Mohsen Alaeian<sup>1</sup>, Bernardo A. D. L. Vignoli<sup>2</sup>, João Victor L. Marchiori<sup>2</sup>, Eduardo P. dos Santos<sup>2</sup>, Gabriel A. Binelli<sup>2</sup>, Rodrigo P. Pedroni<sup>2</sup>, Flavio T. P. Filho<sup>1</sup>

<sup>1</sup> Well Engineering Dept., *Petróleo Brasileiro S/A*

Av. Henrique Valadares, 28, Torre A, 16º andar, 20231-030, Rio de Janeiro/RJ, Brazil

luiznardi@petrobras.com.br, mohsen.alaeian.prestserv@petrobras.com.br, flaviopeixoto@petrobras.com.br

<sup>2</sup>Dept. of Computational Fluid Dynamics, *Wikki Brasil*

Rua Paulo Emídio Barbosa, 485 - Ilha da Cidade Universitária, Parque Tecnológico da UFRJ CETIC - 2º Andar - Sala 301, 21941-907, Rio de Janeiro/RJ, Brazil

bernardo.vignoli@wikki.com.br,

joao.marchiori@wikki.com.br,

eduardo.paiva@wikki.com.br,

rodrigo.pedroni@wikki.com.br

**Abstract.** This study evaluates the use of a retrievable heating tool, deployed via slickline, for dissociating hydrate plugs within a subsea well Christmas Tree (WCT). The focus was on a specific hydrate plug located within the WCT bore, analyzed through multi-phase Computational Fluid Dynamics (CFD) simulations enhanced by adaptive mesh refinement techniques. Findings indicate that a power setting of approximately 3.1 kW is optimal, effectively balancing operational efficiency with safety. This power level maintains temperatures just below the critical threshold of 120°C and achieves complete hydrate dissociation in around three hours. The investigation underscores the importance of precise power calibration and management of its associated uncertainties to ensure the integrity and effectiveness of hydrate dissociation operations.

**Keywords:** CFD, Flow assurance, Hydrate Dissociation

### 1 Introduction

Natural-gas hydrates are ice-like solids that form when a combination of gas and free water is exposed to low temperature and high pressure. If reservoir gas leaks from the lower portion of an oil well to the seabed equipment, it can lead to hydrate formation. To prevent hydrate formation, operators can pump chemical inhibitors, such as Mono ethylene glycol (MEG). However, if hydrate is already formed, one remediation strategy is to elevate local temperatures above hydrate formation threshold (usually 1.8 -11.8°C). If thermal insulation is difficult to achieve, active heating becomes the only option for thermal attack.

This work aims to investigate feasibility of a hydrate dissociation operation, by deploying a retrievable heating tool with slickline, directly above the hydrate plug. Targeted plug under study was formed inside the bore of a subsea well Christmas-Tree. Heater tool would need sufficient power to dissociate the plug by approximation, without exposing Xmas-tree components to temperatures above 120°C.

Since change of state is obligatory for correct modeling of hydrates, CFD models must be multi-phase. A usual strategy to simulate this phenomenon would be breaking down the hydrate phase into different states (gas, liquid and solid) and computing mass transfer of each phase. Computational cost can become elevated with this strategy. The present work aimed to circumvent this cost, by modeling only one hydrate phase. To account for thermodynamical effects of phase change, URANS Navier-Stokes equations were modified, with the addition of source terms to momentum and energy equations.

## 2 Methodology

A method using computational fluid dynamics (CFD) was applied to simulate an operation in which a heating tool is introduced into the Wet Christmas tree (WCT) column. OpenFOAM, an open-source software, was used for these simulations, employing a multiphase solver and additional implementations needed to better understand the dissociation process. Among many possible heat transfer mechanisms, natural convection by a heating tool was chosen to minimize the risk of overheating.

### 2.1 Geometry and domain

Figure 1 (a, b) illustrates the geometry and domain evaluated for the numerical simulations, as well as the positioning of the heating tool inside the Wet Christmas tree (WCT) column. Figure 1(c) shows the fluid domain of interest, considering the initial position of three different phases coexisting inside WCT.

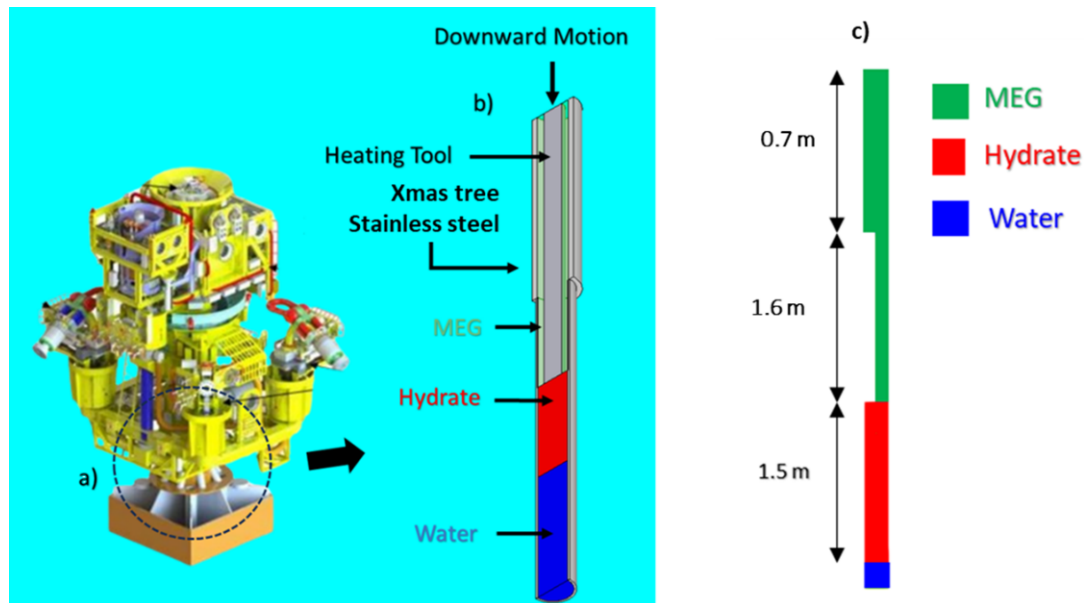


Figure 1. Schematics of hydrate plug inside Xmas tree; (a) location of bore inside Xmas tree, Image adapted from Serrano [1]; (b) Heating tool inside tree bore (c) longitudinal cut of domain, with initial phase distribution

The hydrate plug height is estimated to be 1.5 meters, while the inside diameter of the Wet Christmas Tree (WCT) is about 5 inches. A heating tool that fits the WCT would need to have a maximum outside diameter of 2.5 inches. The tool geometry was considered cylindrical and concentric to the wellbore. The maximum temperature allowed inside the WCT must be  $130^{\circ}\text{C}$  to prevent seal damage to sub-components.

The heating tool would need to be deployed through a slickline or wireline operation until it reaches the top of the hydrate, at approximately 2,000 meters water depth. The domain was considered axisymmetric, as shown in Figure 1 (c). To ensure that the maximum temperatures would only occur inside the domain, final height of domain was chosen as 0.7 m above the initial position of heater top.

### 2.2 Physical problem and mathematical formulation

Heat transfer between bodies was simulated using the Volume-of-Fluid (VoF) method, representing a mixture of three non-miscible incompressible fluids: MEG, water, and hydrate. The non-miscibility hypotheses between MEG and hydrate was made, in accordance to Norgaard and Nygaard [2]. The hydrate was allowed to change phase from solid to fluid. The “icoReactingMultiphaseInterFoam” solver was used, being a transient solver. The VoF approach provides a good representation of the interface capture between the MEG and the dissociated hydrate, both of which are immiscible. A generic property  $\phi$  is defined in the control volume through volumetric

fraction of each phase  $\alpha_i$  as an average weighted by the volume fraction and properties of each phase.

At this point, it is important to highlight that, although the hydrate dissociates, mass transfer is not considered by the solidificationMeltingSource (OpenFOAM [3]) model. Instead, source terms are introduced to express an equivalent flow. The VoF approach allows the resolution of a single set of conservation equations for mass, momentum, and energy, representing the entire fluid field. These are given by the equations (1), (2) and (3).

$$\frac{\partial \rho}{\partial t} + \nabla \cdot (\rho \bar{\mathbf{U}}) = 0 \quad (1)$$

$$\frac{\partial(\rho \bar{\mathbf{U}})}{\partial t} + \nabla \cdot (\rho \bar{\mathbf{U}} \bar{\mathbf{U}}) = -\nabla \bar{P} + \nabla \cdot [\mu_{eff}(\nabla \bar{\mathbf{U}} + \nabla \bar{\mathbf{U}}^T) - \frac{2}{3} \rho k \mathbf{I}] - \mathbf{n}_f \cdot \nabla \rho(T) \mathbf{g} + \sigma \kappa \delta_d \mathbf{n} + \mathbf{S}_d(\alpha, gl) \quad (2)$$

$$\frac{\partial(\rho c_p \bar{T})}{\partial t} + \nabla \cdot (\rho c_p \bar{\mathbf{U}} \bar{T}) = \nabla \cdot (k_{eff} \nabla \bar{T}) + S_h(gl) \quad (3)$$

$\rho$  is the density field,  $c_p$  the specific heat field,  $\mathbf{U}$  the velocity vector,  $P$  the pressure,  $\mathbf{g}$  the gravity vector,  $\mathbf{n}$  the normal vector the interface,  $S_d$  the momentum source term,  $S_h$  the energy source term,  $T$  the temperature,  $k_{eff}$  the effective diffusivity coefficient and  $\mu_{eff}$  the effective viscosity (turbulent and viscous combination). The equations are temporally filtered for Unsteady Reynolds Average Navier-Stokes (URANS) modeling, and the  $k - \epsilon$  model with low Reynolds wall functions is used to model turbulence. To distinguish the phases, volume fraction advection  $\alpha$  is tracked throughout the domain using two transport equations for the phases.

The numerical method for the divergence used the TVD Gauss limitedLinear interpolation scheme present in OpenFOAM for all variables ( $T$ ,  $\alpha$ ,  $k$  and  $\epsilon$ ), with the Gauss linearUpwindV being used for the velocity. Both interpolations are of high order and describe the convective and advective phenomena. For the gradients, the Gauss Linear method was used, which consists of central differences, without orthogonal corrections due to the structured mesh. The discretized equations were solved using the PIMPLE algorithm present in OpenFOAM, which consists of a combination of PISO and SIMPLE, ensuring good convergence (see OpenFOAM [4]).

The third term on the right-hand side (RHS) of eq. (2) represents the buoyancy force due to the density gradient that occurs due to the increase in temperature. The fourth term on the RHS is the liquid-liquid interfacial tension force. This work used  $\sigma = 0.02\text{N/m}$  as the value of the interfacial tension between water, MEG, and hydrate (mainly composed of methane), for a pressurized region of 260 bar (the hydrostatic pressure in the Christmas tree), as per (Norgaard and Nygaard [2]).

$$S_{d0}(gl) = -C \frac{(1 - gl)^2}{gl^3} U \quad (4)$$

$$S_d(\alpha, gl) = \frac{1}{\alpha_h / (S_{d0} - \epsilon) - (1 - \alpha_h) / \epsilon} + \epsilon \quad (5)$$

$$S_h(gl) = \rho L \frac{\partial gl}{\partial t} + \epsilon \quad (6)$$

$\epsilon$  is a constant to be calibrated,  $\alpha_h$  is the hydrate phase fraction,  $L$  is the latent heat of fusion of the hydrate,  $gl$  is the phase fraction of the dissociated hydrate,  $C$  is a constant of the resistance of the porous medium. The momentum term in eq. (4) is a numerical device that represents the resistance of a porous medium in the interface region, as a function of the volumetric fraction of dissociated hydrate ( $gl$ ) present in the control volume (Rad [7]; Voller and Prakash [8]). For solid hydrate ( $gl = 0$ ), the source term grows exponentially, making the flow behave like a solid (frozen), and for  $gl = 1$ , the source term cancels out, allowing the liquid to flow freely (Rad [7]; Voller and Prakash [8]). Values between 0 and 1 express an equivalent porous medium resistance, representing a phase change transition region (Hauschildt et al [9]). In the present work, the momentum source term  $S_{d0}(gl)$  was mathematically modified and implemented to couple it to VoF. The source term  $S_{d0}(gl)$  became now a function of multiple variables as  $S_d(\alpha, gl)$ , including  $\alpha_h$  and  $gl$ , written by the formulation of eq. (5), being a jump

harmonic, widely used for interfacial modeling (Deoclecio [5]; Zotelle [6]). The values of the constants  $C$  and  $\varepsilon$  were calibrated to ensure an ideal smoothing and resistance curve at the interface, both having a value of  $1 \times 10^7$ . For the energy source term, its formulation remains as originally obtained in Rad [7] and described by eq. (6), expressing the additional latent heat necessary to cause dissociation of the solid hydrate.

### 2.3 Mesh Generation and Dynamic Mesh

The phase change routine was implemented in the CFD code with the addition of a source term to the momentum and energy equations of the Multiphase Solver. This source term was designed to account for the latent heat of hydrate and would only act on hydrate phases.

A high level of mesh refinement was necessary at the interface between the hydrate and other fluids. An adaptive refinement mesh technique was implemented for accuracy purposes, significantly reducing computational cost. In addition, a moving grid routine was employed, allowing a dynamic representation of the tool descent. The VoF method successfully accounted for interfacial tension between phases, as well as buoyancy generated by density gradients within the mixture.

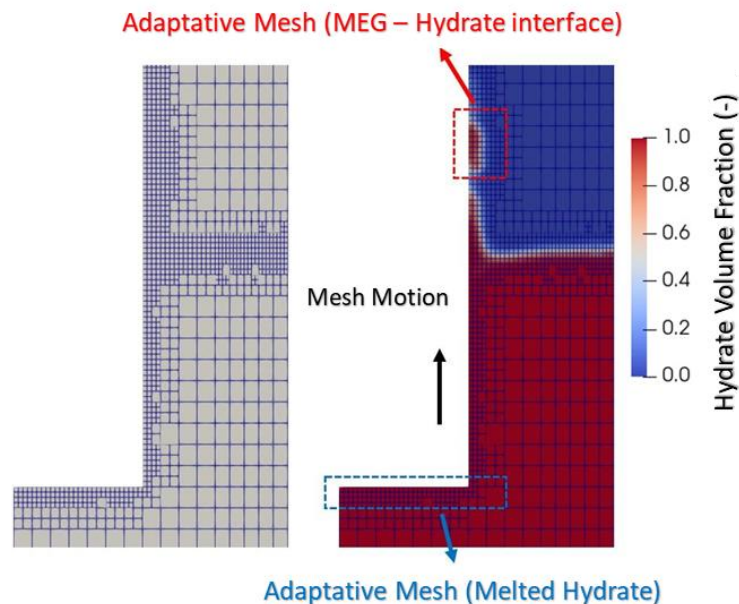


Figure 3. Moving and adaptive mesh to accurately describe the system.

The mesh is generated in an axisymmetric domain using the blockMesh tool, which has the advantage of creating a structured, fully hexahedral mesh.

### 2.4 Operation Conditions and Setup

A range of cases was simulated in a context where the WCT is located in the pre-salt, and dissociation temperature of the hydrate at this depth is  $26^\circ\text{C}$ , according to Sloan and Koh [10]. The powers at the wall of the heating tool, as listed in Table 1, were used. Each power is associated with a descent velocity to keep up with the hydrate's dissociation rate. The descent velocity was calculated based on the conservation of energy associated with latent heat, where  $Q = \dot{m}H$ . According Grupta et al. [11], the latent heat for hydrate is  $H = 436 \text{ kJ/kg}$ . The value of  $\dot{m}$  was obtained through static simulations evaluating the dissociation rate adjacent to the tool tip.

**Table 1.** Tool power associated with its descent velocity.

Tool power (kW)	Tool descent velocity (mm/s)
1.5	0.075
2.0	0.100
2.5	0.125
3.0	0.150
4.5	0.225

### 3 Results and Discussion

This section presents the results and analyses of the simulation of hydrate dissociation, focusing on the dissociation rate and operational time, maximum temperature analysis and corresponding power.

#### 3.1 Hydrate dissociation and operational time

The results for the 4,500 W case are presented in Figure 4a. The left side of the figure displays the volume fraction of the hydrate field, while the right side shows the dissociated hydrate field. As the tool descends continuously, the dissociated hydrate just below the tool rises up the side wall due to higher temperatures and the dissociation process, transitioning to a liquid state in this region of contact. The red areas in the right-side image highlight the detachment of a hydrate bubble, which is also observed in Figure 4a.

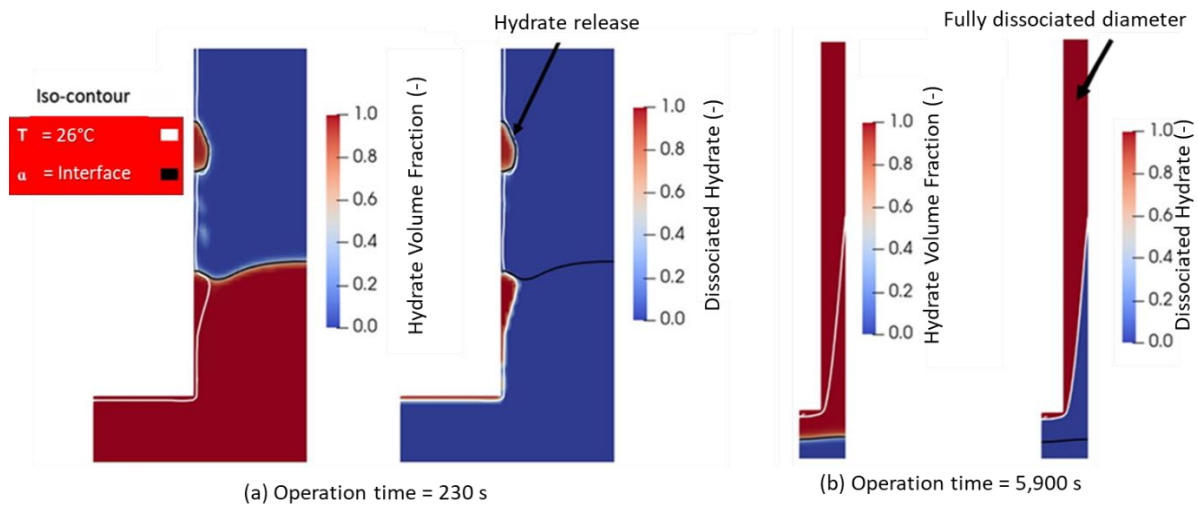


Figure 4. Hydrate field and hydrate field with 4500 W power.

Figure 4b illustrates the hydrate dissociation process at moments close to the end of the operation (5,900 seconds, covering almost the entire 1.5-meter block). A well-defined dissociation front around the tool (marked by the white line) can be seen, extending across the entire diameter of the internal column of the Xmas Tree and rising to regions higher up the tool where temperatures are higher. This demonstrates the capability to dissociate the hydrate along the entire inner wall. Results indicate that the tool needs to descend slightly more than 1.5 meters to ensure complete dissociation of plug. Black lines in Figure 4 (b) delineates the interfaces between the hydrate phase and formation water.

#### 3.2 Power estimation of the heater tool

Maximum allowable temperature inside WCT is typically around  $T_{\max} = 130^{\circ}\text{C}$ . Adding a safety margin of  $10^{\circ}\text{C}$  was, one can define maximum tolerated temperature as  $T_{\max,2} = 120^{\circ}\text{C}$ . The temperature distribution for the extended domain is evaluated in Figure 7. An important point to highlight is that the global maximum form

temperature occurs at the top of the tool, during transient regime of the heating. For heights above tool top ( $h > 1.6\text{m}$ ), temperatures tend to decrease, due to the absence of heat sources in the surroundings.

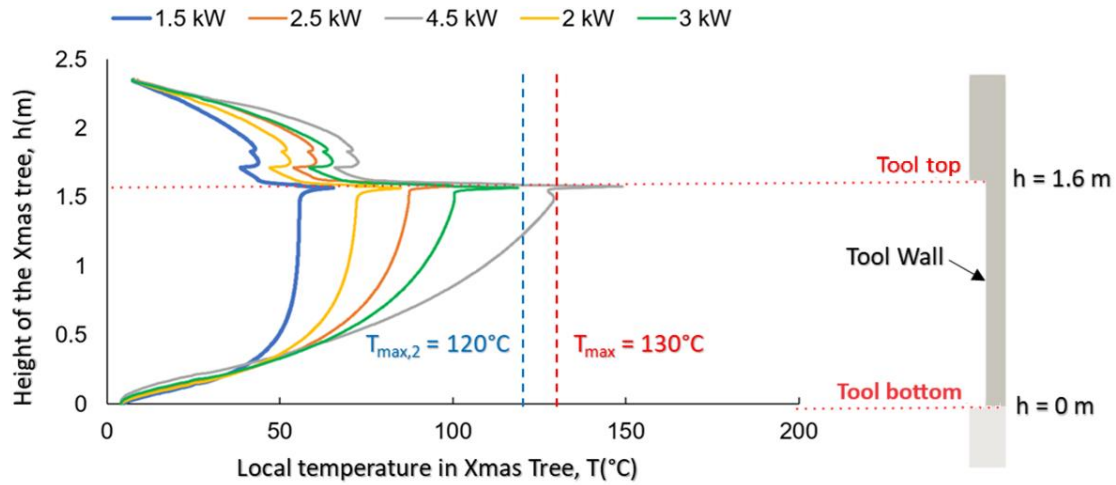


Figure 7. Temperature distribution along the Tree at the end of the operation for extended domain.

Figure 8 shows a correlation between maximum temperature and power. The corresponding power for  $T_{\max,2} = 120^\circ\text{C}$  obtained from the correlation presented in Figure 8 is  $P = 3.1\text{ kW}$ .

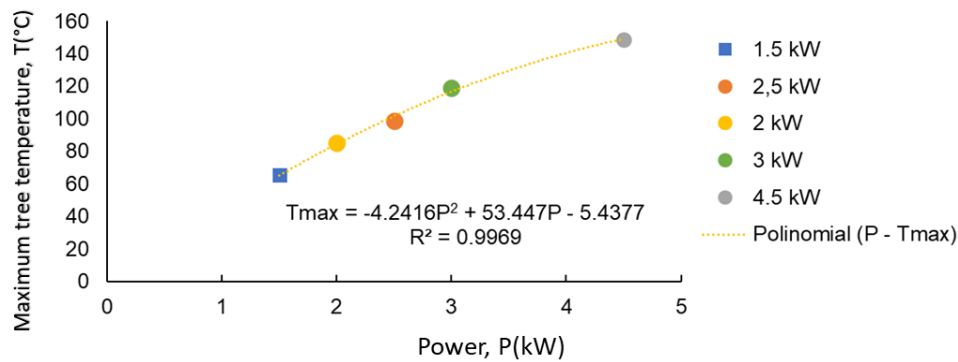


Figure 8. Relationship between maximum WCT temperature and tool power.

It is crucial to understand the power uncertainty of the heating tool due to its significant impact on temperature perturbations around the maximum allowable temperature. This power resolution should be carefully considered, to ensure safety margin for the operation.

#### 4 Conclusions

The feasibility of utilizing a heating tool to dissociate hydrate plugs in a Wet Christmas Tree (WCT) was evaluated through numerical and analytical studies, considering power levels ranging from 1.5 kW to 4.5 kW. Results indicate higher power values are less time-consuming but can lead to over-heating of WCT, if inner temperatures rise above  $130^\circ\text{C}$ .

The model showed that the maximum temperature tends to occur near the top of the tool, which can be explained by the natural convection phenomenon. This type of convection has less chances of over-heating WCT, since all the heated fluid will tend to exit the tree. Simulations indicated that power levels up to 3.1 kW could be used safely, with an estimated mission time of 2 h 45 min.

A correlation was established between dissipated power and maximum temperature in WCT. This correlation can offer a guide for appropriate tool selection. Operators are encouraged to monitor local temperatures during the

dissoiation process. Further simulations can be performed after these temperatures are measured, to mitigate thermodynamical uncertainties present in the model.

**Authorship statement.** The authors hereby confirm that they are the sole liable persons responsible for the authorship of this work, and that all material that has been herein included as part of the present paper is either the property (and authorship) of the authors or has the permission of the owners to be included here.

## 5 References

- [1] Serrano, P. J. C., Projeto de Ferramenta de Assentamento de Buchas de Desgaste na Superfície. Universidade Federal do Rio de Janeiro – Campus Macaé, Macaé, 2017.
- [2] H. Norgaard and L. Nygaard, *Measurement and Calculation of Surface Tension of Oil, Gas and Glyco*, Master's Thesis, Norwegian University of Science, 2014.
- [3] OpenFOAM: API Guide v2112; Available on [https://www.openfoam.com/documentation/guides/latest/api/icoReactingMultiphaseInterFoam\\_8C.html](https://www.openfoam.com/documentation/guides/latest/api/icoReactingMultiphaseInterFoam_8C.html)
- [4] The OpenFOAM Foundation, OpenFOAM v6 C++ Source Code Guide; Available on: [https://cpp.openfoam.org/v6/classFoam\\_1\\_1fv\\_1\\_1solidificationMeltingSource.html](https://cpp.openfoam.org/v6/classFoam_1_1fv_1_1solidificationMeltingSource.html)
- [5] Deoclecio, L. H. P., *Drop Rise and Interfacial Coalescence Initiation in Complex Materials*, PhD diss., Universidade Federal do Espírito Santo (UFES), 2023.
- [6] Zotelle, A.C., *Numerical Study of the Effects of Viscosity Ratio and Capillary Number on The Displacement Efficiency in Homogeneous and Heterogeneous porous media by Newtonian, viscous-thinning and viscous-thickening fluids*, Universidade Federal do Espírito Santo (UFES), 2023.
- [7] Rad, M. T., Solidificationmeltingsource: A built-in fvoption in openfoam® for simulating isothermal solidification. Springer International Publishing, Cham, p. 455–464, 2019. Available on: <[https://doi.org/10.1007/978-3-319-60846-4\\_32](https://doi.org/10.1007/978-3-319-60846-4_32)>.
- [8] Voller, V.R., Prakash, C., “A fixed grid numerical modelling methodology for convection-diffusion mushy region phase-change problems”. *International Journal of Heat and Mass Transfer*, vol. 30, Issue 8, pp 1709-1719, 1987, Available on: [https://doi.org/10.1016/0017-9310\(87\)90317-6](https://doi.org/10.1016/0017-9310(87)90317-6)
- [9] Hauschildt, J. et al., Methane Hydrate and Two-Dimensional Fluid Transport Model: Comparison with Blake Ridge Chlorinity Measurements. *Transp Porous Med*, Germany, 2013. Available on: DOI 10.1007/s11242-013-0225-z.
- [10] Sloan, E. D., Koh, C. A. *Clathrate Hydrates of Natural Gases*. CRC Press, 2008. <https://doi.org/10.1201/9781420008494>
- [11] Gupta, A. et al. Measurements of methane hydrate heat of dissociation using high pressure differential scanning calorimetry. *Chemical Engineering Science*, USA, 2008. Available on: doi:10.1016/j.ces.2008.09.002